Tests on a Master Gap Working at Atmospheric Pressure

D.V. Bayes +)

IPP/4/40 February 1967

INSTITUT FÜR PLASMAPHYSIK

GARCHING BEI MÜNCHEN

INSTITUT FÜR PLASMAPHYSIK

GARCHING BEI MÜNCHEN

Tests on a Master Gap Working at Atmospheric Pressure

D.V. Bayes +)

IPP/4/40 February 1967

+) attached Staff from Culham Laboratory, England

Die nachstehende Arbeit wurde im Rahmen des Vertrages zwischen dem Institut für Plasmaphysik GmbH und der Europäischen Atomgemeinschaft über die Zusammenarbeit auf dem Gebiete der Plasmaphysik durchgeführt.

IPP/4/40 D.V. Bayes

Tests on a Master Gap Working at Atmospheric Pressure

February, 1967 (in English)

Abstract

A master gap has been tested and graphs of jitter and delay against charging voltage are presented for two gap ratios, different numbers of cables connected and different values of centre electrode capacitance. In addition the pulse rise-time has been plotted against charging voltage and against the number of cables connected.

Index

Illustrations

1. Introduction

A redesigned master gap with epoxy resin insulation has been made, with the centre electrode introduced assymetrically i.e. off the main axis, as shown in the sectioned view in fig 1. The gap can accommodate up to 24 cables, and the influence of the number of cables on some characteristics of the gap has been examined.

It is intended that the gap will be triggered using only the pulse from a normal 14 kV hydrogen thyratron unit and the consequent limitation of the working range is accepted because of the simplicity of the trigger circuit.

2. Tests and the presentation of results

The test circuit diagram is shown in fig 2. and initially only one 11 meter output cable was connected. From this circuit it is clear that the jitter of the thyratron and delay units are included in the measurements at the gap. However, tests proved that the jitter for these units was too small to be measured on the fastest time base of the oscilloscope (2o nsec/cm) and this arrangement was therefore justified by its convenience.

The gap ratio was set geometrically to 1:2 and the ratio checked using an electrostatic voltmeter, the total static breakdown voltage was 42.5 kV. The cable was charged and the gap used to short-circuit the cable, the resulting 2 x V output pulse was measured at the open-circuit end of the 11 meter cable.The jitter and delay of the gap were measured down to 16.5 kV, using 1o consecu tive shots at each voltage to measure the jitter.

The rise-time of the pulse was measured for each charging voltage by measuring the slope of the central portion of the rise, and by reference to the time and amplitude calibrations of the oscilloscope, giving the value in kV/nsec. This method was adopted in preference to the more usual 1o % to 9o % value because it was quicker and more appropriate because the trigger pulse feeds

through onto the output pulse, making it difficult to know exactly where to take the 1o % value. This is especially true when only a few cables are connected. The graphs of jitter, delay and rise-time are plotted in figs 3, 4 and 5 respectively.

With 6 output cables connected, a single measurement of the rise-time at 4o kV charging voltage (94 % static) was taken and plotted in fig 6.

Using 12 output cables, the jitter, delay and rise-time were measured and the results plotted in igs 3, 4 and 5.

With 18 cables connected a single measurement of the rise-time at 4o kV charging voltage (94 % static) was taken and plotted in fig 6.

The cable number was then increased to the maximum number of 24, when jitter, delay and rise-time were again measured and are plotted in figs 3, 4, and 5 respectively.

From the above results, fig 6 shows the rise-time as a function of the number of cables connected, with the charging voltage held constant.

The gap ratio was changed to 2:3 which increased the static breakdown to 46.o kV. The jitter and delay were measured for different charging voltages and plotted in figs 7 and 8. On these graphs are also plotted the corresponding results for a gap ratio of 1:2 for comparison. This result may be a little misleading because the static breakdown voltages were not the same, which means that the ratio of trigger voltage to charging voltage was more favourable for the ratio 1:2 because of the lower static breakdown voltage.

The influence of the length of the trigger gap (irradiation gap) on the jitter of the main gap was briefly examined. The results, plotted in fig 9, indicate that a very small gap gave the lowest overall jitter in this geometry. If the gap was reduced to zero, the jitter of the main gap would be very high, working without

irradiation, hence there must be a knee value very close to zero gap. However it is difficult to set a very small gap in this assembly and it is impractical to go smaller than o.1 mm.

The influence of the centre electrode capacitance on the overall jitter is shown in fig 1o and again in fig 11 where two values of the decoupling capacitor are used. The fig 12 shows the comparison of the jitter against voltage characteristics for the original and the optimised values of decoupling and centre electrode capacitance, for the 1:2 gap ratio. Fig 13 gives the same comparison for the 2:3 gap ratio. It is clear that increasing the centre electrode capacitance will load the trigger pulse and slow down the initial swing of the electrode and may affect the breakdown of the first part of the gap. On the other hand, the larger capacitance improves the overswing of the electrode after the first part of the gap has broken down, thereby giving a higher voltage for the breakdown of the second part. A compromise must be made between these two conditions and should be investigated for each new geometry because the geometry and the amplitude and shape of the trigger pulse are important parameters.

Using the optimised values of decoupling and centre electrode capacitance, a comparison of the two gap ratios is given in fig 14. Comparing this with fig 7, when the original values of c were used, it is only in the case of the 2:3 gap ratio that the improvement is marked. The corresponding graph of delay against voltage for the gap ratio is shown in fig 15.

3. Conclusions

This investigation is incomplete, there are many more measurements which could be made to supplement those already taken, but which the present circumstances do not allow. The above results are therefore presented at their face value as a record, rather than as a fully concluded report.

4. Acknowledgements

The design of the master gap by Mr. G. Klement and the provision of the test facilities by the High Voltage Technology Group, is hereby acknowledged.

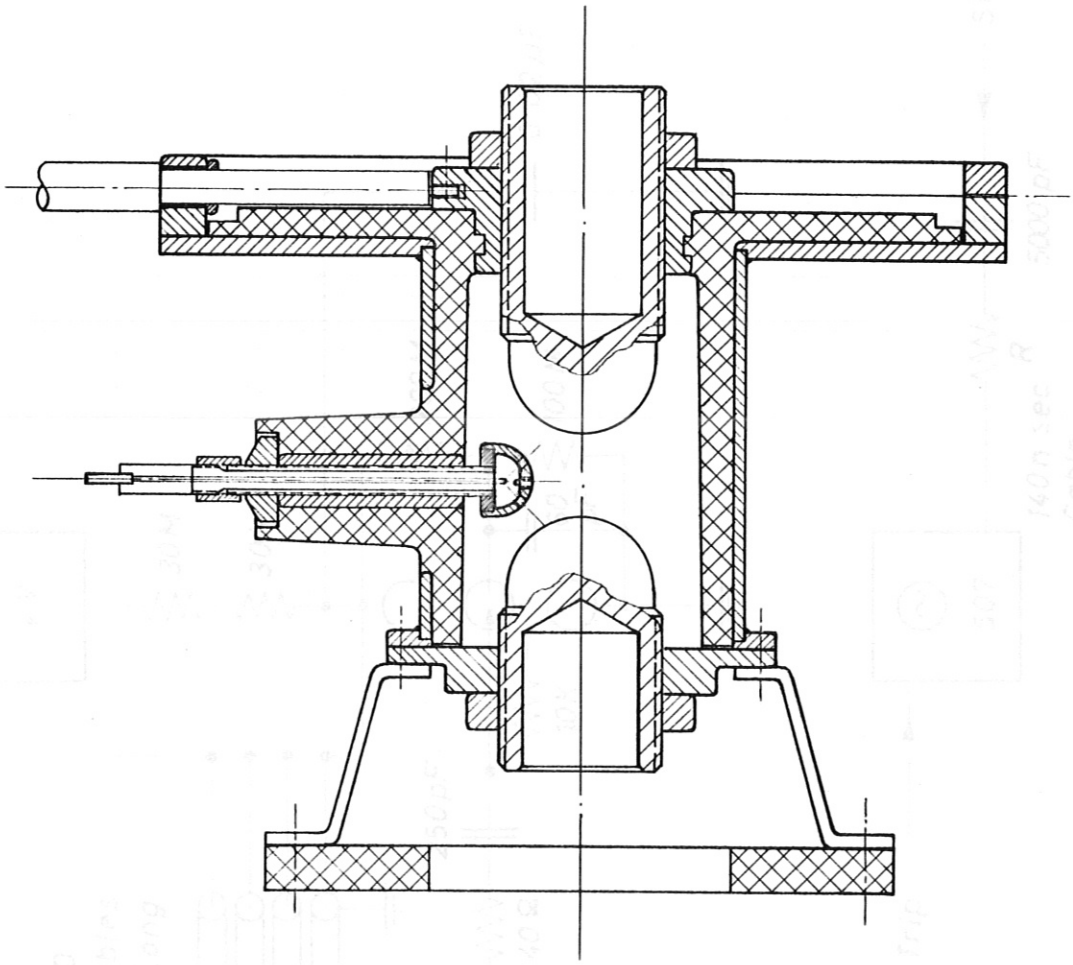

Sectioned view of 1B 164 - 0 drawn ½ scale

Fig.1 Sectioned view of the master gap

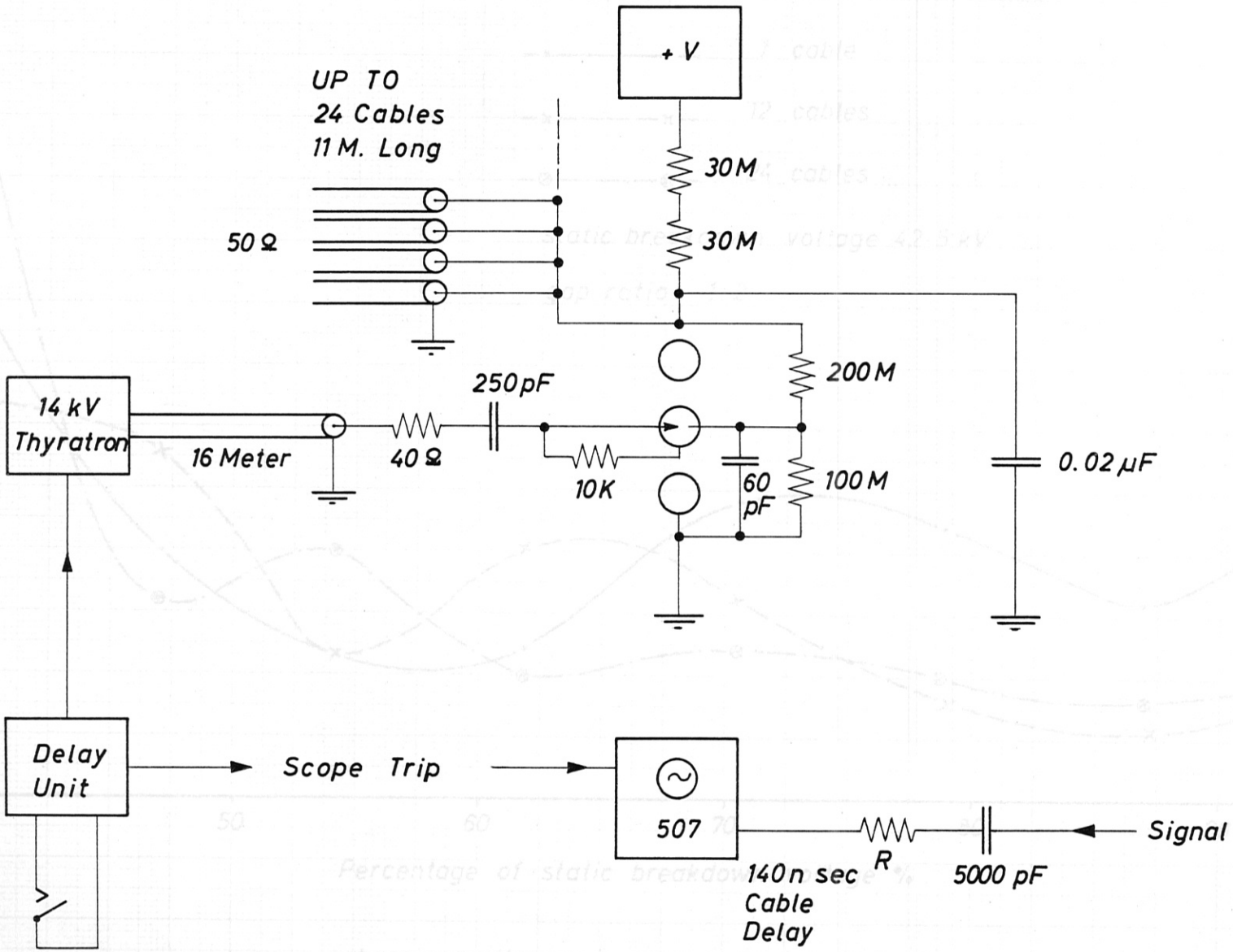

Fig. 2 Test circuit diagram

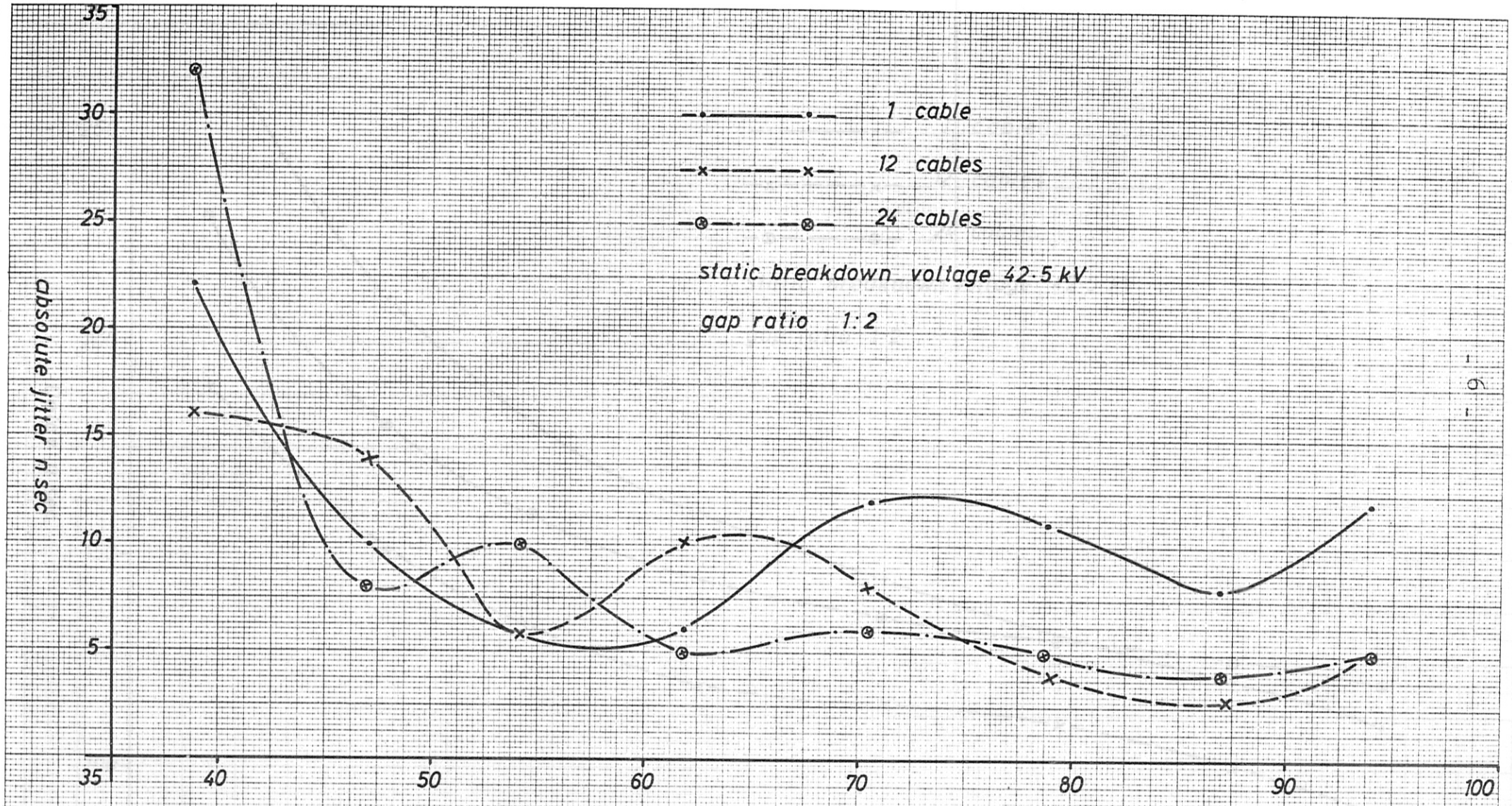

Fig. 3 Graph of jitter against $\frac{\text{charging voltage}}{\text{static breakdown voltage}}$ %

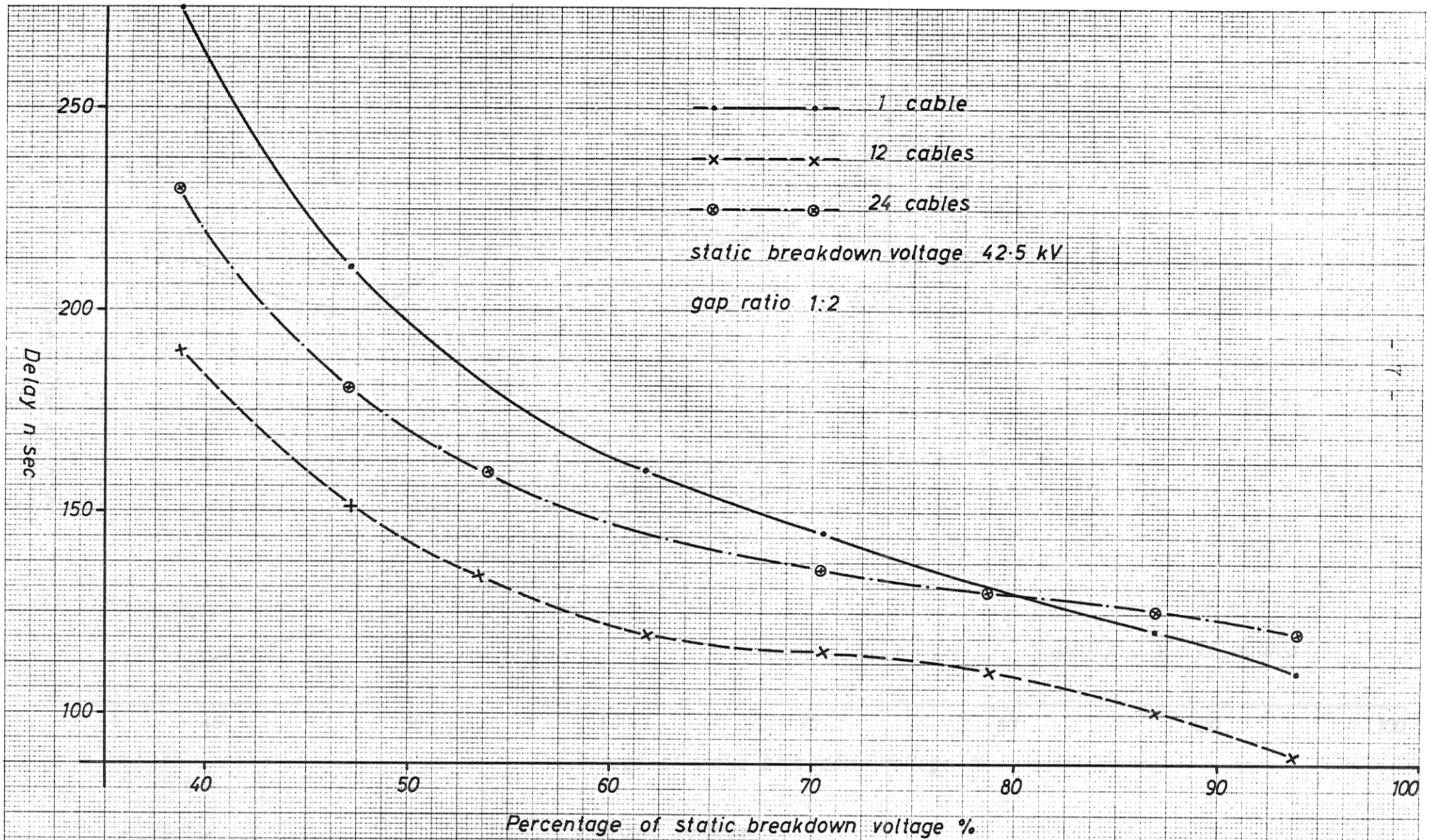

Fig. 4 Graph of delay against $\frac{\text{charging voltage}}{\text{static breakdown voltage}}$ %

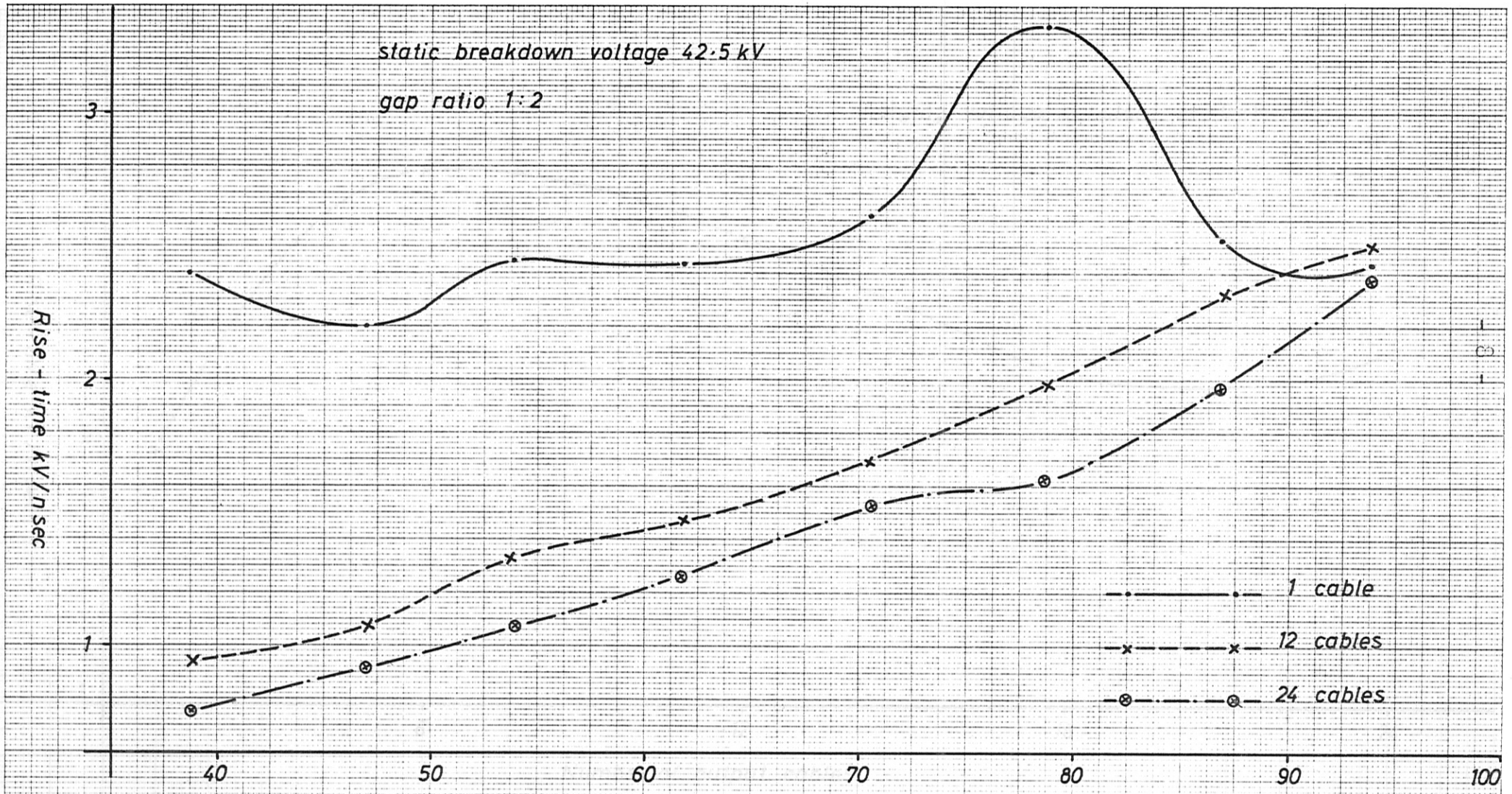

Fig. 5 Graph of rise - time against $\frac{\text{charging voltage}}{\text{static breakdown voltage}}$ %

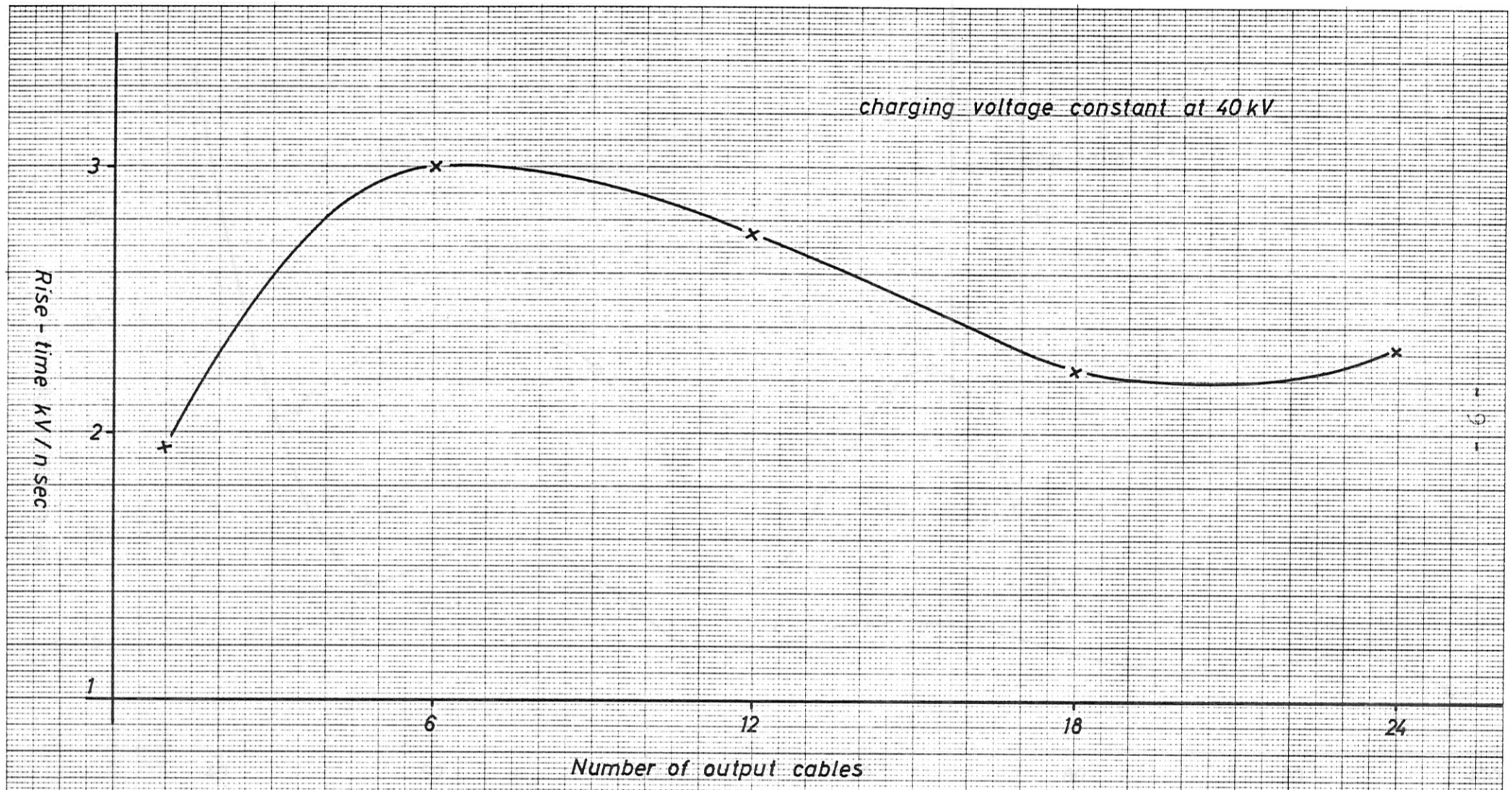

Fig. 6 Graph of rise - time against number of output cables

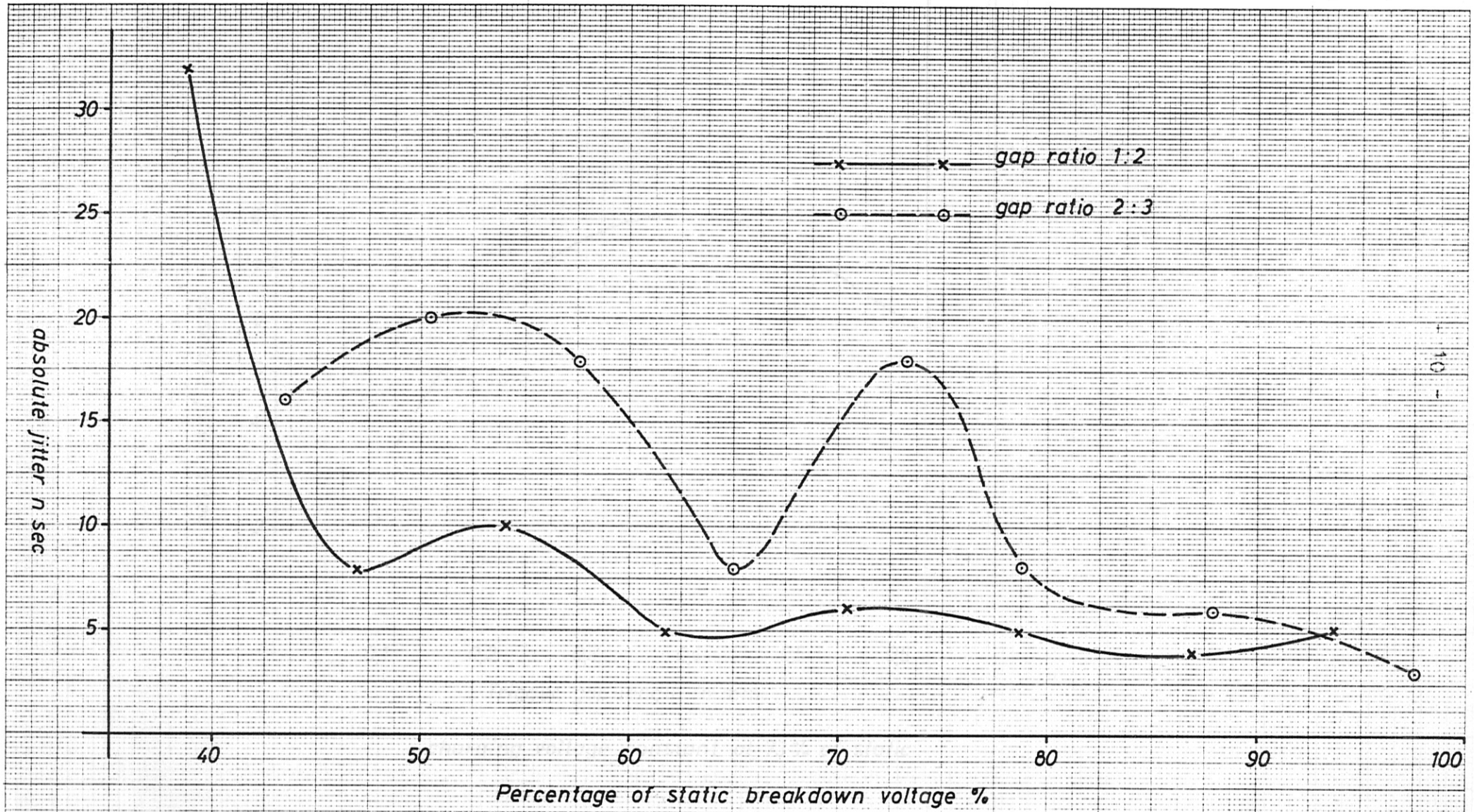

Fig. 7 Graph of jitter against $\frac{\text{charging voltage}}{\text{static breakdown voltage}}$ % for two values of gap ratio

Fig. 9 Graph of jitter (total breakdown) against trigger gap length

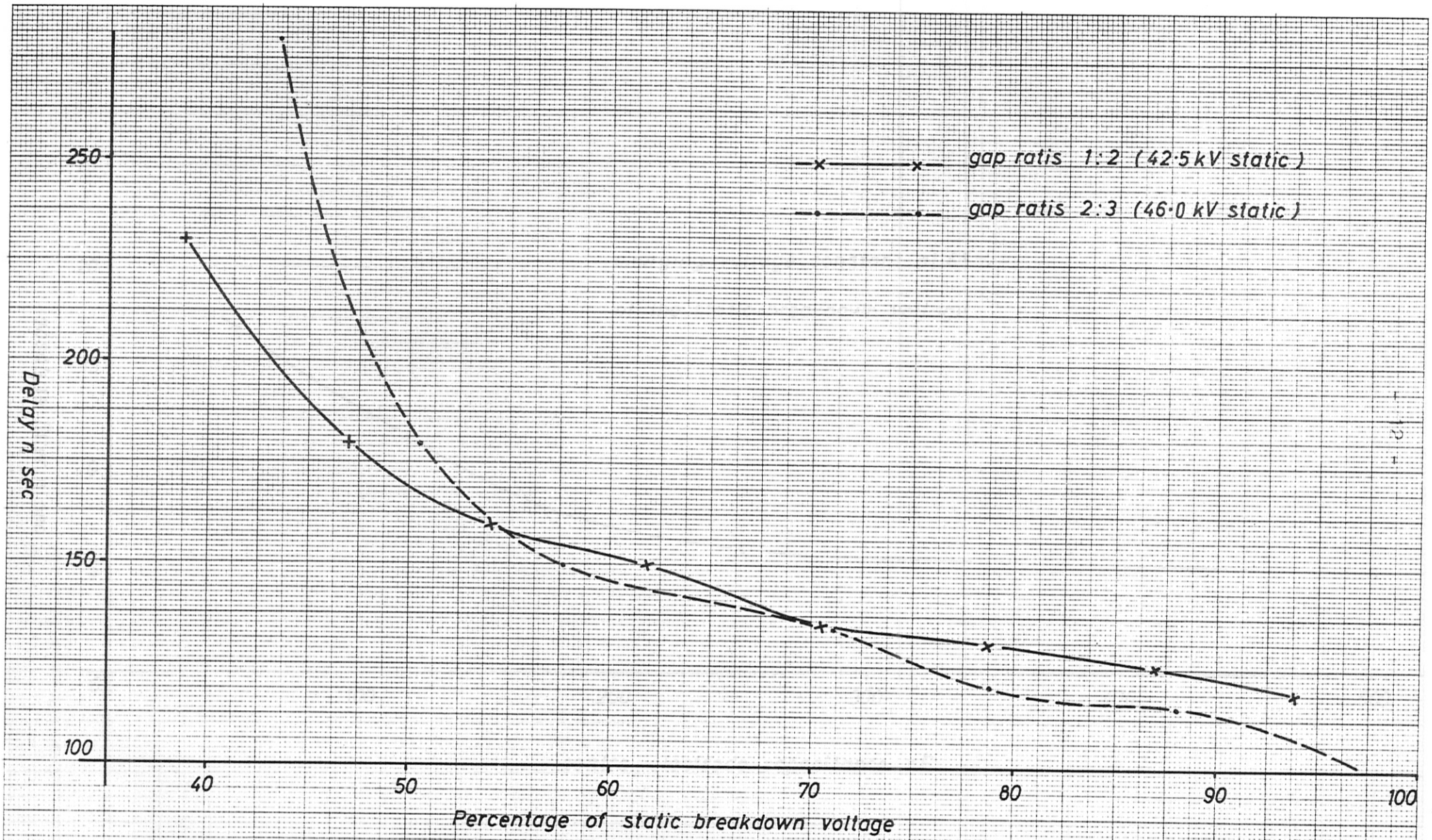

Fig. 8 Graph of delay against $\frac{\text{charging voltage}}{\text{static breakdown voltage}}$ % for two gap ratios

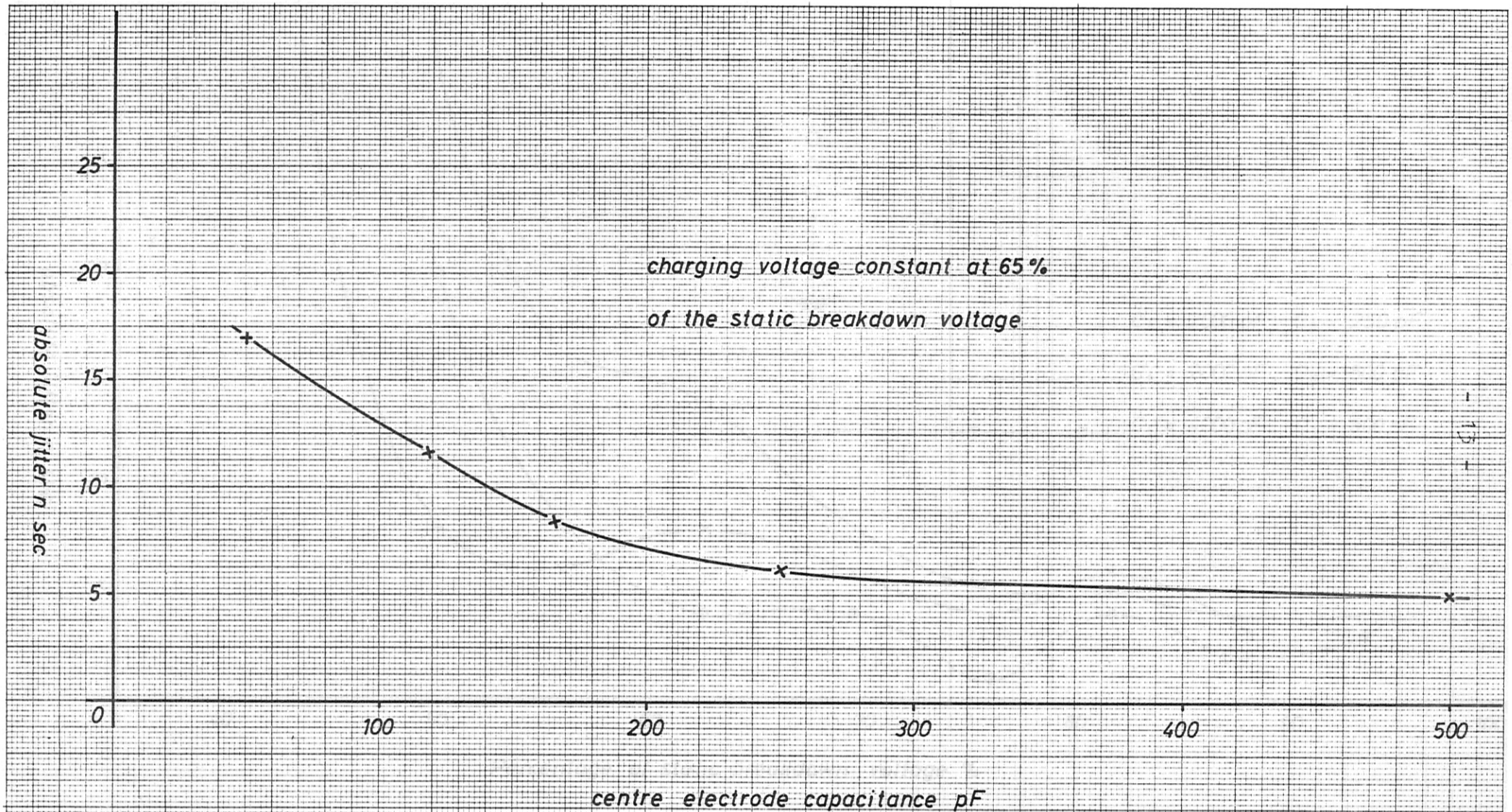

Fig. 10 Graph of jitter against centre electrode capacitance

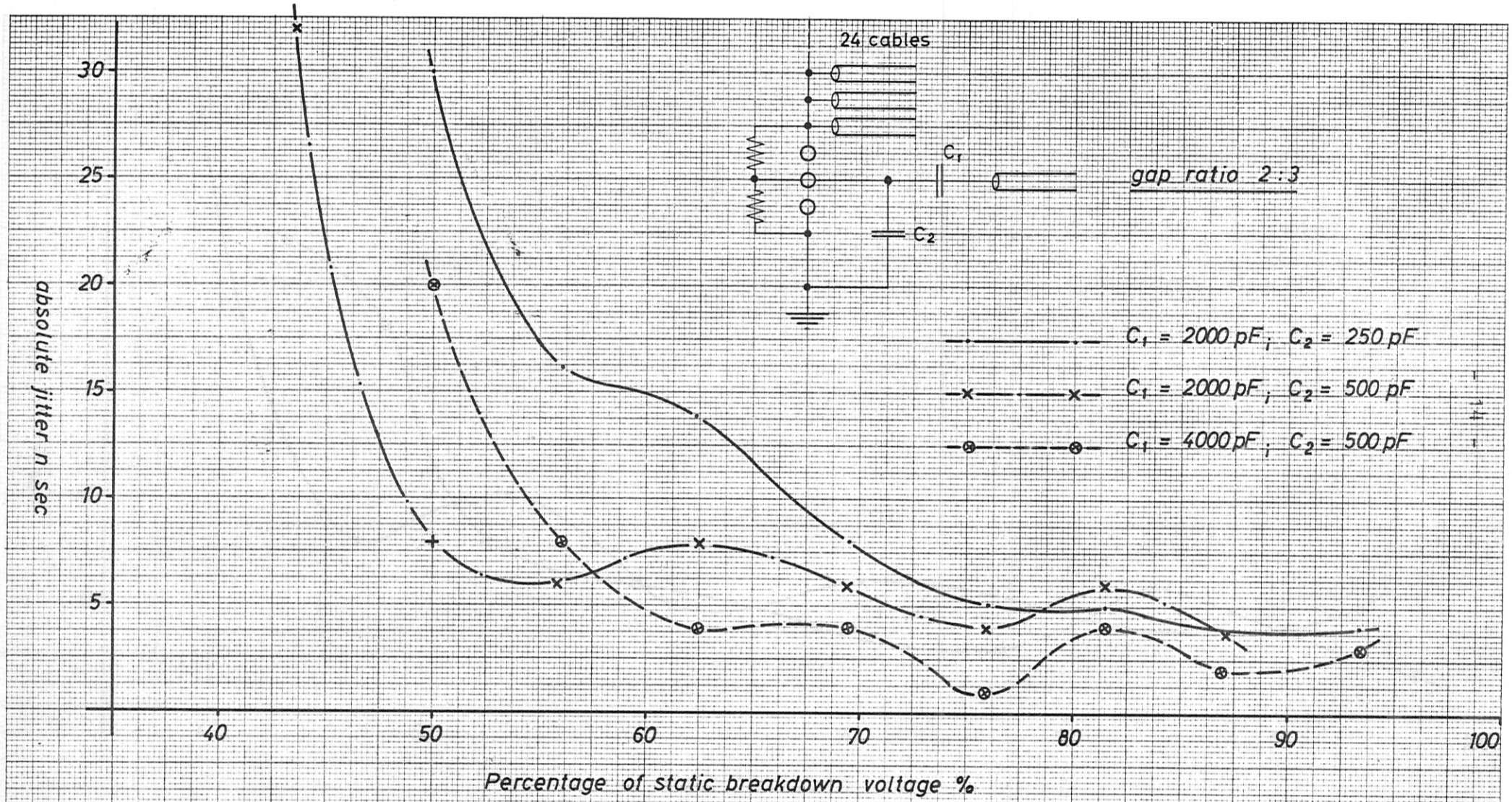

Fig. 11 Graph of jitter against $\frac{\text{charging voltage}}{\text{static breakdown voltage}}$ % for different values of C

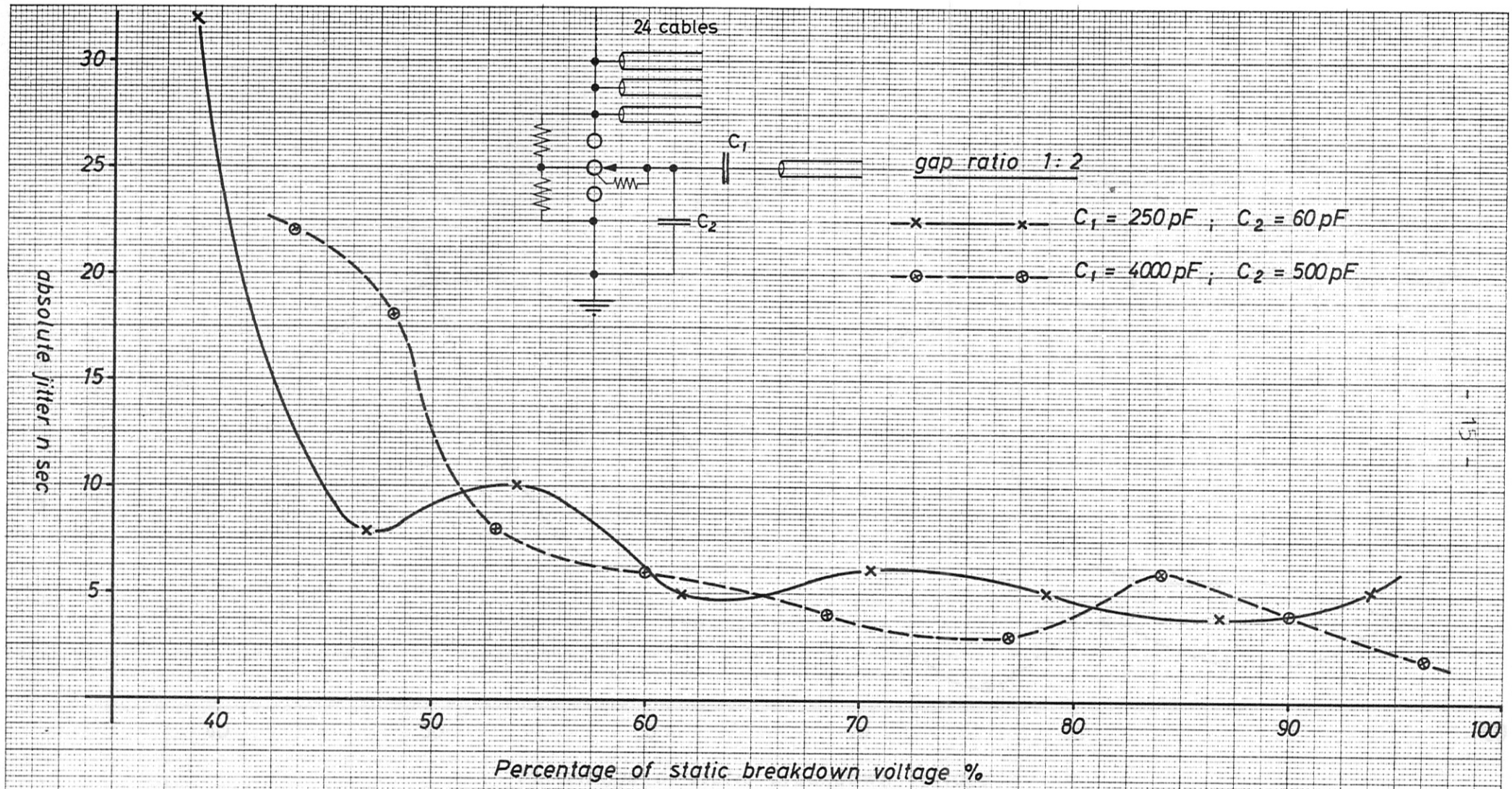

Fig. 12 Comparison of original and optimised values of C for 1:2 gap ratio

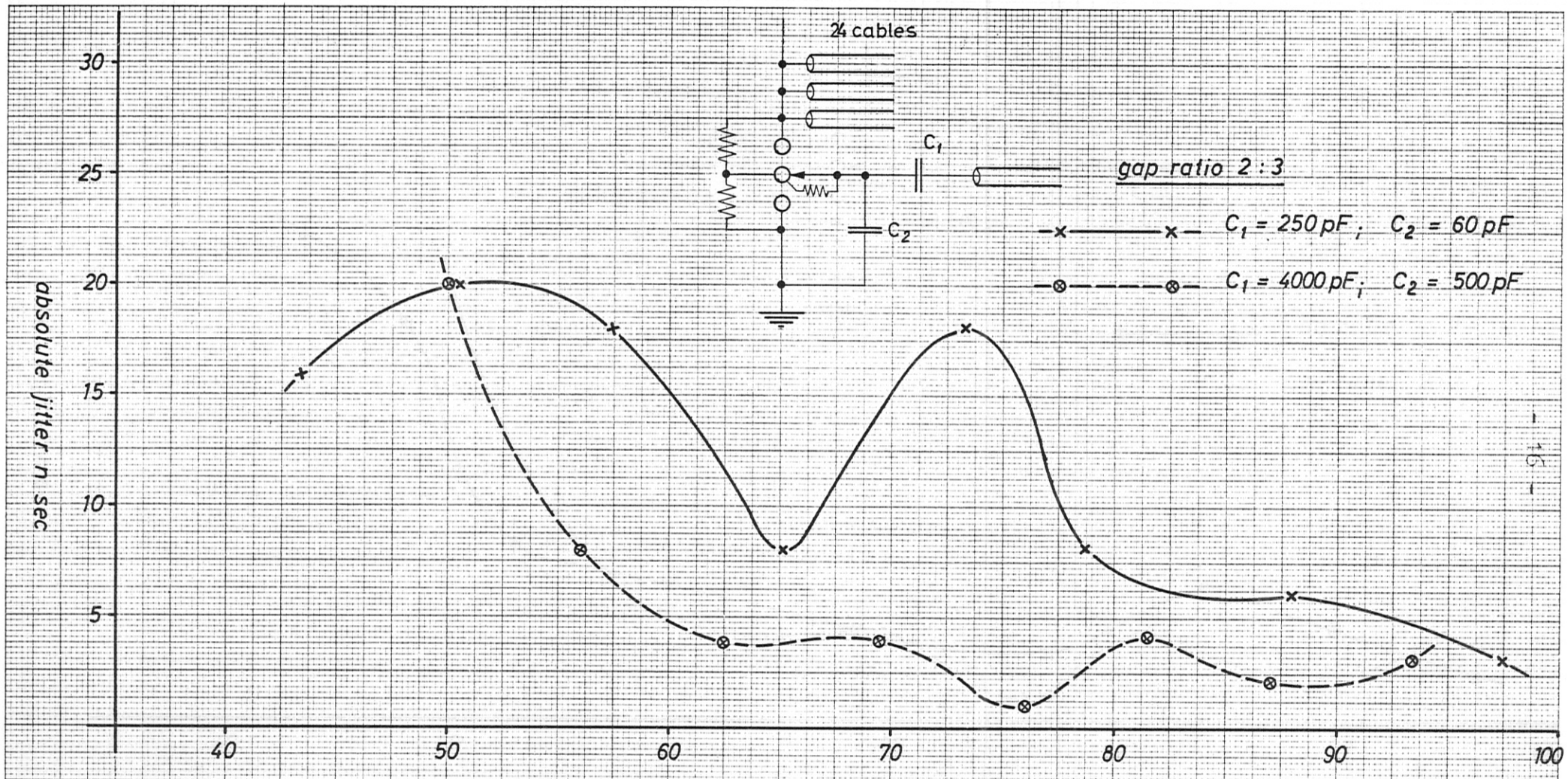

Fig. 13 Camparison of original and optimised values of C for 2 : 3 gap ratio

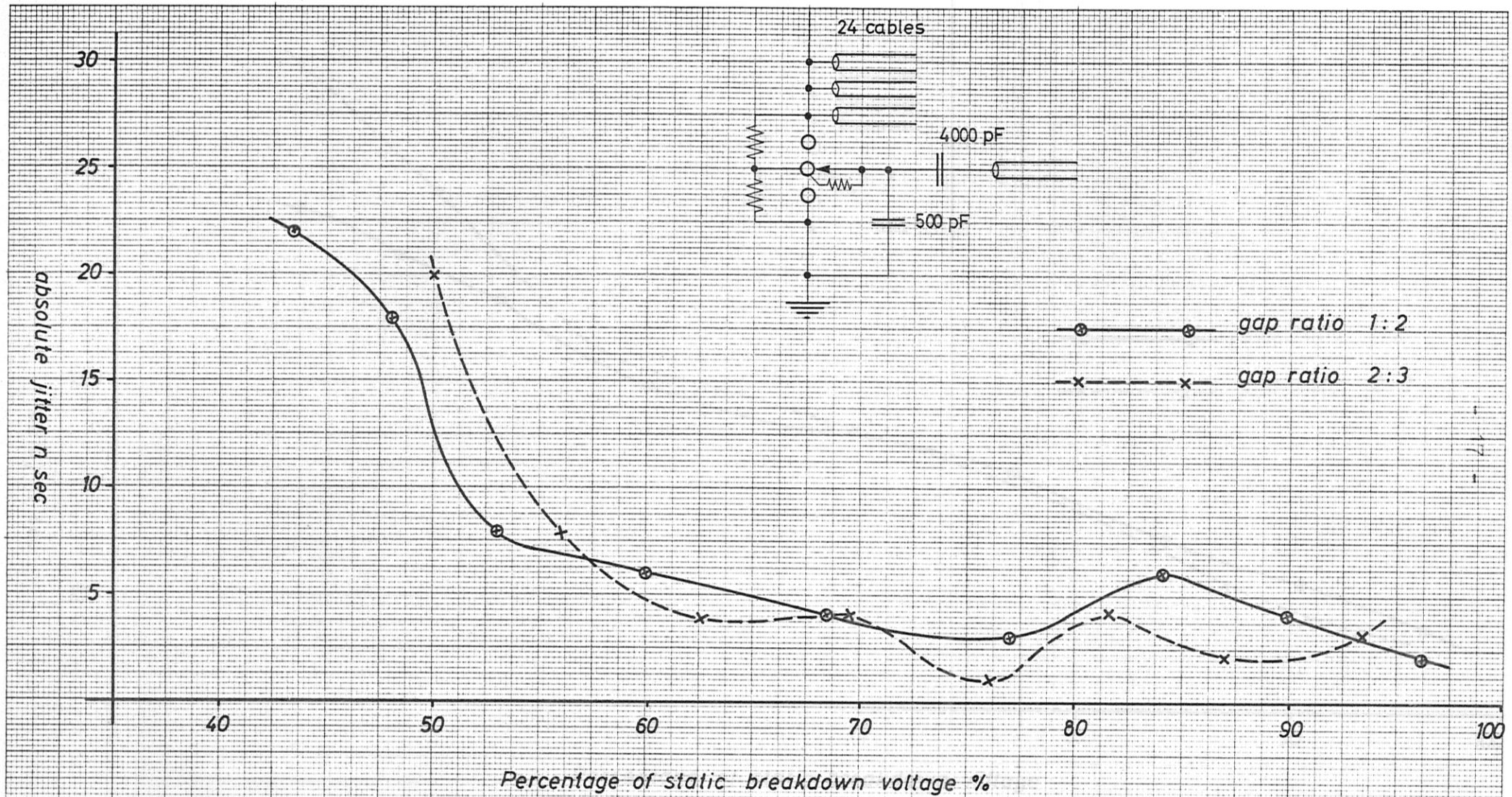

Fig. 14 Comparison of gap ratios with optimised values of C

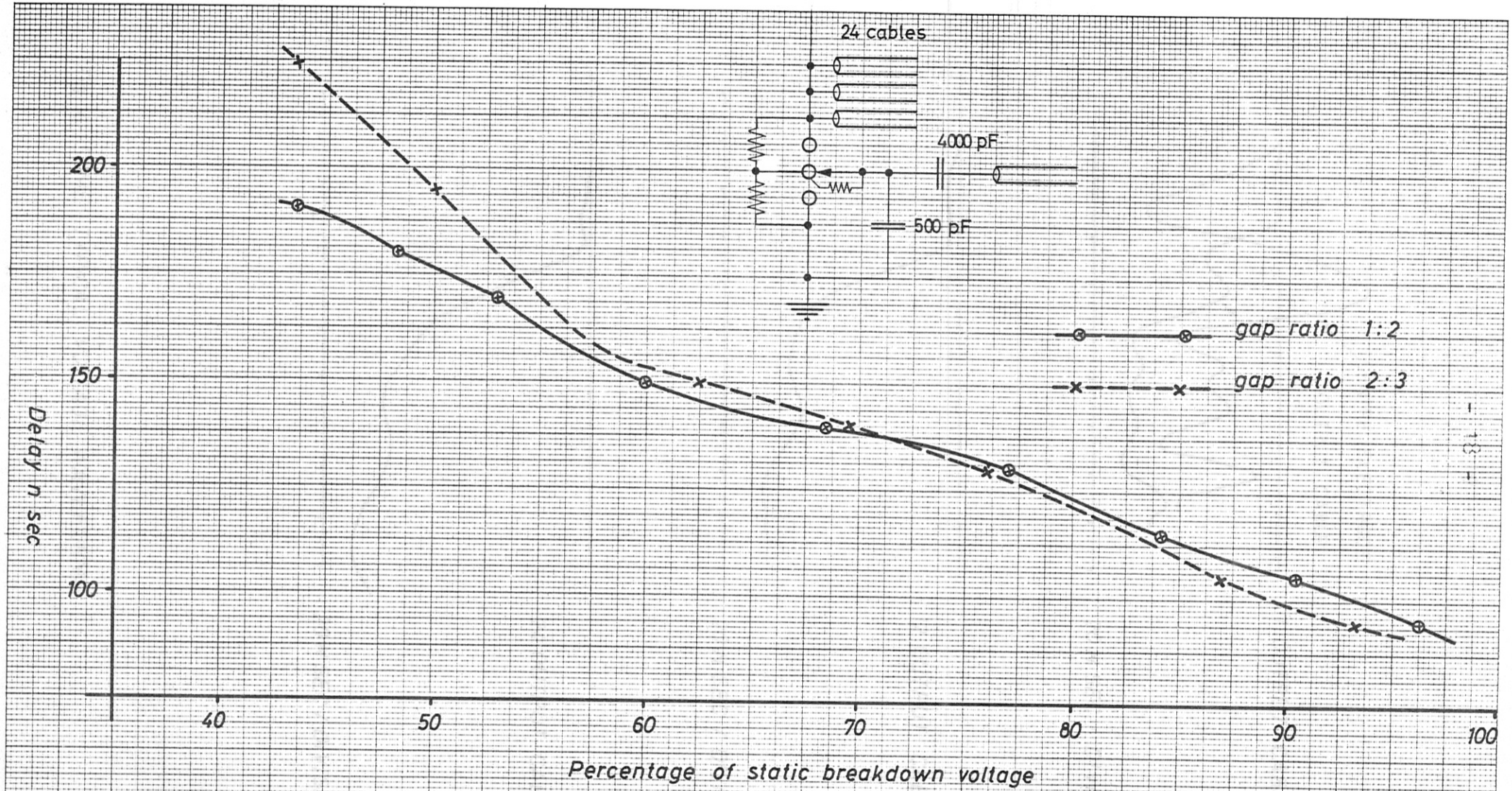

Fig. 15 Comparison of the delay against voltage for gap ratios 1:2 and 2:3

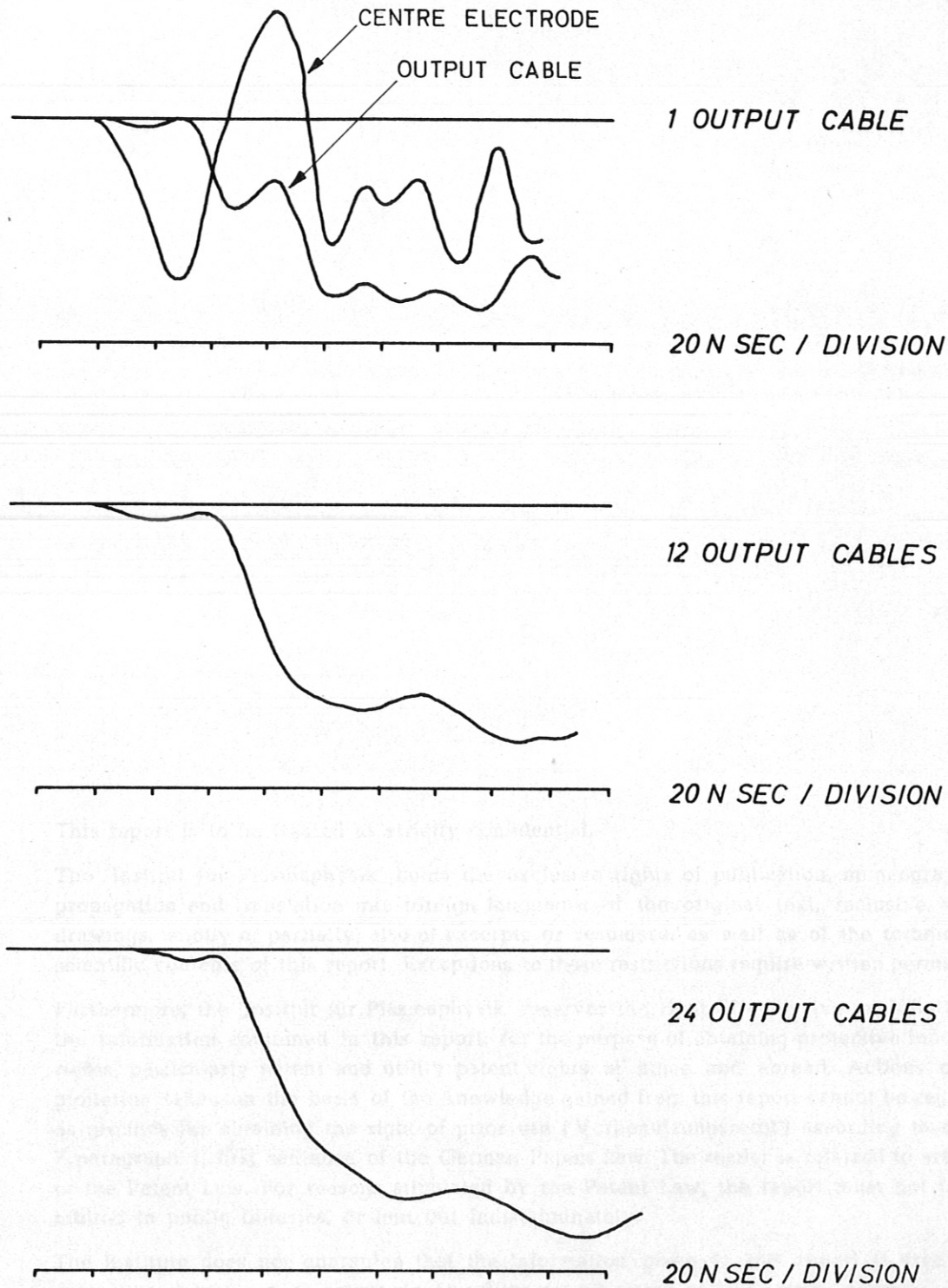

Fig. 16 SOME TYPICAL VOLTAGE WAVEFORMS